Old Dominion University

ODU Digital Commons

Investigation of Matrix Effects on the Furnace Atomic Absorption Signals of Chromium, Nickel and Selenium

Susan Marie Viet
Old Dominion University

INVESTIGATION OF MATRIX EFFECTS ON THE FURNACE

ATOMIC ABSORPTION SIGNALS OF CHROMIUM,

NICKEL AND SELENIUM

by

Susan Marie Viet
B.S. May 1978, Old Dominion University

A Thesis Submitted to the Faculty of
Old Dominion University in Partial Fulfillment of the
Requirements for the Degree of

MASTER OF SCIENCE
(ANALYTICAL CHEMISTRY)

OLD DOMINION UNIVERSITY
May, 1984

Approved by:

Director: Patricia A. Pleban

Billy T. Upchurch

Robert L. Ake

ABSTRACT

INVESTIGATION OF MATRIX EFFECTS ON THE FURNACE
ATOMIC ABSORPTION SIGNALS OF CHROMIUM,
NICKEL AND SELENIUM

Susan Marie Viet
Old Dominion University, 1984
Director: Dr. Patricia A. Pleban

The flameless atomic absorption signals of chromium,
nickel and selenium are subject to matrix interferences
arising from inorganic salts and anions commonly found
in urine. The effects of such salts on the atomic
absorption signals were investigated using Polarized
Zeeman Effect background correction in conjunction with a
detector/readout system capable of resolving absorbance
signals in 18 msec readings. Both optical temperature
control and current temperature control were employed for
each analysis. Peak area, peak height, peak shape and
appearance time were compared for matrix-free standards
and matrix-containing standards.

The influence of the inorganic salts on the metal
analyses was found to be significant. Calcium and mag-
nesium enhanced chromium, nickel and selenium signals,
although it appeared the cations acted via different
mechanisms. Suppression of the signals by phosphate,
nitrate or sulfate was most likely caused by absorption

from diatomic species formed in the furnace. Such species exhibit structured background and produce Zeeman spectra in a magnetic field. Although use of optical temperature control improved sensitivities and detection limits, the effects of matrix components were the same whether optical or current control was used.

Urine could not be analyzed directly for the metals studied. Adjustments of the furnace heating program should improve the analyses but dilution, matrix modification and the method of standard additions would still be required.

ACKNOWLEDGEMENTS

TABLE OF CONTENTS

LIST OF TABLES

LIST OF FIGURES

INTRODUCTION

Detection of extremely low concentrations of chromium, nickel and selenium in urine is of clinical importance. Chromium plays a role in glucose tolerance and is found in urine at levels of less than 1 ppb (1). Urinary nickel is a measure of nickel intoxication, normal values being as low as 4 ppb (2). Selenium is an essential cofactor for glutathione peroxidase and is present in urine at concentrations of 20-200 ppb (3).

Flameless atomic absorption is the most widely used method for analyzing trace metals. The technique, however, is subject to a variety of matrix interferences. The most common background correction system eliminates broadband absorption by placing a secondary, continuum source, usually a deuterium arc lamp, at right angles to the primary source and chopping the two beams so that they pass alternately through the sample space. Since background is absorbed by both beams, electronic ratioing of the signals reduces the effect of background absorption. Deuterium corrected atomic absorption (DCAA) requires exact optical alignment and intensity matching. Correction is limited to the more intense region of the arc continuum. Discrete spectral interferences are still

1

present since the resolving power of normal spectrometers is too low to separate rotational spectra of some diatomic molecules (4).

A relatively new correction system based on the Polarized Zeeman Effect should compensate for some of the problems associated with continuum correctors (5). Figure 1 shows the basic components of the Polarized Zeeman atomic absorption (PZAA) system. Differential absorption by perpendicular and parallel components of the source radiation, due to the polarization character-istics of the electronic transitions of the analyte metal in an applied external magnetic field, forms the basis. for background correction. Correction is performed at the desired wavelength and optical alignment is not critical. Because the same source beam is used, correction capability is similar at all wavelengths, provided the analyte possesses a resonance line showing a suitable Zeeman effect. Absorption of the source by structured background can be eliminated as long as it does not exhibit a Zeeman effect and occurs outside the Zeeman splitting frequencies (6).

Improper instrumental design may add to the "apparent" matrix interference. A recently-described problem with flameless atomic absorption techniques has been the use of slow response time detector-readout systems. Lundberg and Frech (7) have shown that matrix
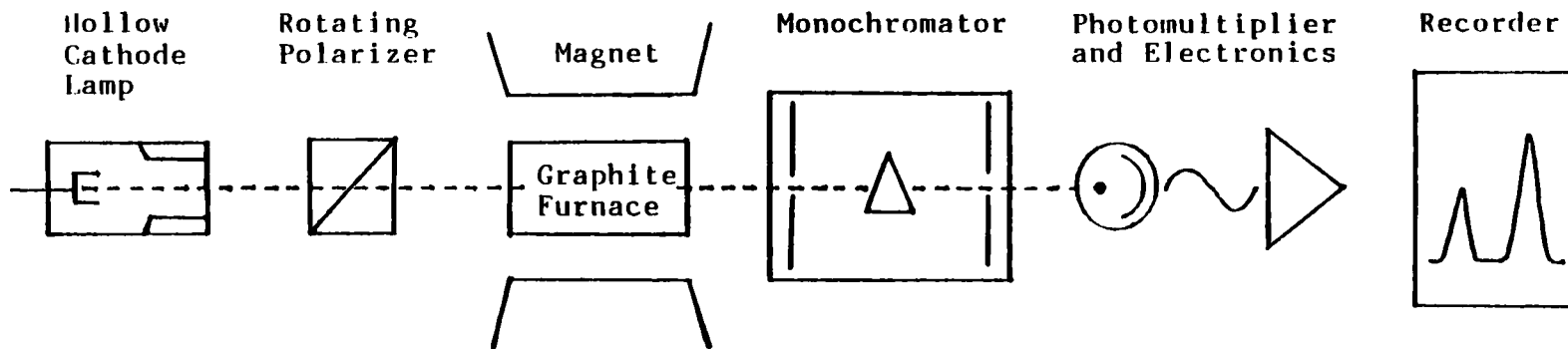
Figure 1. Block diagram of the Polarized Zeeman Atomic Absorption Spectrophotometer

salts affect the vaporization characteristics of the analyte by changing the atomization interval and/or the rate of atom formation. They conclude that the overall time constant of the readout system should be 0.1 times the temporal half-width of the peak and determine 10-12 msec to be sufficient in most analyses. Many systems in common use resolve peaks in 200-300 msec readings.

Van de Broek and co-workers (8) found that another instrumental variable, the rate of furnace heating during atomization, affected peak shape and sensitivity. Two methods of controlling atomization temperature have been employed in commercial instruments. The first, current control, exercises temperature control by maintaining a constant current flow through the graphite furnace. This results in a steady, sigmoidal rise in the furnace temperature over the atomization period, as shown in Figure 2a. The second method, optical control, adjusts the current to maintain a constant optical emission from the furnace. Figure 2b illustrates the almost instantaneous rise in furnace temperature obtained with optical control. Faster atomization of the analyte increases analyte absorption, thus enhancing peak height and peak area measurements since the signal-to-noise ratio is improved.

Matrix effects can be examined by studying changes in peak characteristics when the matrix is present (7).

2a.

CURRENT CONTROL

2b.

OPTICAL CONTROL
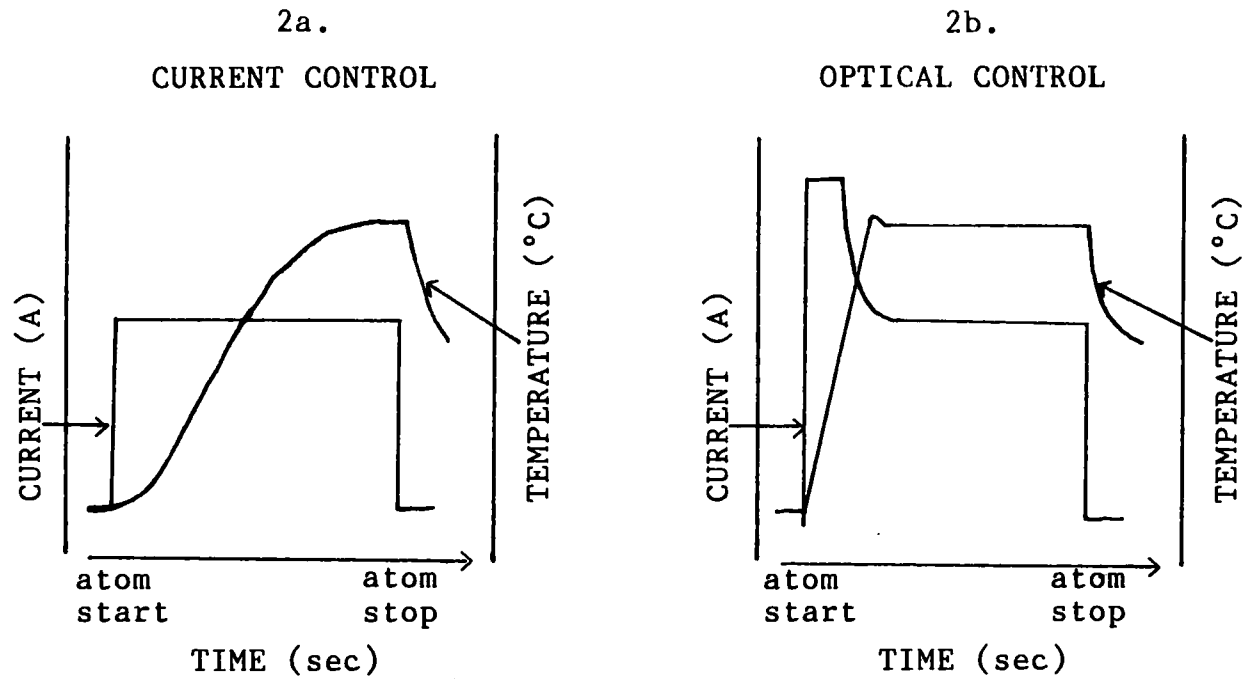
Figure 2. Comparison of current and temperature versus time during atomization for each control system studied (Courtesy of Hitachi, Ltd.)

If a matrix variable changes the atomization interval and/or the rate of atom formation, the peak height of the atomic absorption signal will be altered. If the matrix changes only the atomization interval, the peak area will be altered. A shift in appearance time means that the formation mechanism of analyte atomis has changed due to the new chemical environment, e.g., different partial pressure arising from interfering elements such as oxygen and chlorine. Peak shape can indicate several things. A negative dip in the baseline when the analyte is not present can reflect inadequate background correction. Double peaks or shoulders on the peak suggest the formation of more than one analyte species during atomization.

The objective of this research was to study the effects of some common anions and salts present in urine on the atomic absorption signals of chromium, nickel and selenium when determined by Zeeman background corrected flameless atomic absorption. The detector/readout system resolved peaks in 18 msec readings, sufficient sampling time for peaks with half-widths of 180 msec or greater. Peak shape, peak area, peak height and appearance times of matrix-free standards were compared to matrix-containing standards. Temperature control using both constant current and constant optical emission was employed for each analysis in order to assess the influence of heating rate on apparent matrix effects.

HISTORICAL REVIEW

The majority of matrix effect studies have been
carried out on DCAA systems. A study similar to this
research examined the effects of a variety of cations and
anions present in wastewater on lead, copper and cadmium
analyses (9).

Stein and associates (10) studied the determina-
tion of selenium by DCAA in fresh and estuarine waters.
They found that sodium, sulfate, chrloide and nitrate
depressed the selenium signal while calcium, magnesium,
nickel and iron enhanced the signal. Thompson and Allen
(11) showed that selenium could be analyzed in nutritional
supplements containing more than 30% lipid following
suspension in an acidic emulsion of a diluted, block-
digested sample. Strong interferences by aluminum,
potassium, sodium and sulfate on the analysis of arsenic,
a metal chemically similar to selenium, have been
observed (13).

Chromium and nickel determinations have also been
studied by DCAA in a wide range of matrices. Alder and
Hickman (14) found that up to 2% nitric acid, hydrochloric
acid and hydrogen peroxide have no effect on chromium or
nickel signals. However, various cations affect the

analysis of nickel differently, depending on which acid is present (15). In 0.2$\underline{M}$ HCL: aluminum, cobalt and iron depressed the signal; potassium, sodium, magnesium and calcium had no effect. In 0.2$\underline{M}$ HNO_3: calcium, magnesium and cobalt depressed the signal; potassium, sodium, iron and aluminum had no effect. Depression of the nickel signal has been observed in the Ni-$CuCl_2$ system, whereas in the Ni-$PbCl_2$ system, no depression occurs (16). Magnesium chloride and magnesium sulfate have been reported to enhance the chromium signal, while sodium sulfate and calcium chloride showed no effect (17). Both chromium and nickel have been determined in serum by standard additions (18) and directly using oxygen as a matrix modifier during the ashing cycle (19). Use of the L'vov platform and addition of ammonium phosphate has been shown to reduce common matrix effects to within 10% of the original response for chromium and nickel (20). Krasowski and Copeland (21) compared effects for chromium using a Woodriff furnace and a carbon rod atomization (CRA) furnace. Sodium chloride, sodium perchlorate and ammonium chloride suppressed the signal less than 5% in the Woodriff furnace, while the results were as much as 90% low for the CRA furnace.

Relatively few matrix studies have been conducted using Zeeman background correction. Pleban and Perason (22) have shown that all nitrate salts exhibit no effect

on lead signals when analyzed by PZAA. They found suppression of the lead signal by the chloride salts of sodium, potassium, magnesium and calcium and by phosphate. Cadmium was analyzed directly in whole blood and urine (23).

Polarized Zeeman background correction is reported to correct up to 1.7 absorbance seconds. Initial studies for chromium analyses of sludge and biological fluids showed the background interference to be eliminated using this correction method (24). Chromium and nickel have been analyzed in 0.2$\underline{M}$ NaCl and 0.2$\underline{M}$ HCl without interference (25). Guthrie et al. (26) attributed the many problems associated with analyzing chromium in urine to the inadequacy of the conventional deuterium background correction and suggested using the Zeeman correction system.

Vickrey and Buren (27) used PZAA to study the effects on the selenium signal of metal ions coated on the surface of the graphite furnace. Lanthanum, nickel, zirconium and tantalun enhanced the absorption signal.

Limited investigations using adequate response times to study peak characteristic changes as a result of matrix materials have been reported. Oscilloscope tracings of manganese in the presence of magnesium sulfate showed a difference in appearance times and peak heights (28). Analysis of peaks for copper and manganese

in the presence of calcium nitrate, magnesium nitrate and magnesium sulfate showed that no generalization of the effects via a similar mechanism was possible. Recorder tracings resolved in 10 msec readings for lead prepared in sodium nitrate or sodium chloride matrices showed appearance times and peak heights to vary when different salts were present (7).

EXPERIMENTAL METHODS

Apparatus

Measurements of chromium, nickel and selenium
solutions were made using a Polarized Zeeman Effect
Flameless Atomic Absorption Spectrophotometer, Model 180-
70, equipped with a dual-pen, fast-response recorder,
Model 056, and an auxiliary optical pyrometer (N.S.A.
Hitachi, Ltd., Mountainview, CA). The instrument stored
the furnace signal in memory (resolved in 18 msec
readings). By recalling the stored peak, the true signal
could be recorded.

All glassware was Kimax (Owens Illinois, Toledo,
OH). Stock solutions were stored in polyethylene
bottles (Nalge Co., Rochester, NY). Working standards
were prepared in polypropylene test tubes (Falcon,
Oxnard, CA). Automatic Eppendorf micropipets (Brinkman
Industries, Westburg, NY) and Finn pipets (Finn Pipette,
KY, Finaldn) were used for all pipetting steps. Disposable
pipet tips were rinsed to remove contamination by
pipetting deionized water three times before use.

A 1000 ppm chromium stock solution was prepared by
dissolving 1.4146 grams of primary standard potassium
dichromate in 500 ml of deionized water. Nickel stock

11

solutions, 1000 ppm and 5000 ppm, were prepared by dissolving 0.2500 grams of primary standard grade nickel powder (SPEX Industries, Inc., Metuchen, NJ) in a minimum volume of Ultrex nitric acid (J. T. Baker Chemical Co., Phillipsburg, NJ) and diluting to 250 ml and 50 ml volumes, respectively. Commercially-prepared 1000 ppm stock selenium atomic spectral standard was used (J. T. Baker Chemical Co., Phillipsburg, NJ).

The following reagent grade acids were diluted with deionized water to give stock solutions of 25,000 ppm chloride, 40,000 ppm phosphate, 40,000 ppm sulfate and 20,000 ppm nitrate: HCl, H_2SO_4 (Mallinckrodt, Inc., St. Louis, MO) and HNO_3, H_3PO_4 (J. T. Baker Chemical Co., Phillipsburg, NJ). Anion and cation stock solutions were stored at 4°C.

Magnesium stock solutions were prepared from each of the following reagent grade salts by dissolving appropriate amounts in deionized water to give 1000 ppm magnesium: $MgSO_4 \cdot 7H_2O$, $MgCl_2$ (Mallinckrodt, Inc., St. Louis, MO) and $Mg(NO_3)_2 \cdot 6H_2O$ (General Chemical Co., New York, NY). A 1000 ppm magnesium stock solution was prepared as the dihydrogen phosphate salt by adding phosphoric acid dropwise to reagent grade magnesium oxide (J. T. Baker Chemical Co., Phillipsburg, NJ) until dissolution was near completion, then adding deionized

water and adjusting the pH of the solution to 5.9 with phosphoric acid.

Calcium stock solutions were prepared from each of the following reagent grade salts by dissolving appropriate amounts in deionized water to give 1000 ppm calcium: $Ca(NO_3)_2 \cdot 4H_2O$ (MCB Manufacturing, Inc., Darmstadt, Germany) and $CaCl_2$ (J. T. Baker Chemical Co., Phillipsburg, NJ). A 1000 ppm calcium stock solution was prepared as the dihydrogen phosphate salt by adding phosphoric acid dropwise to reagent grade calcium oxide (J. T. Baker Chemical Co., Phillipsburg, NJ) until dissolution was near completion, then adding deionized water and adjusting the pH of the solution to 5.0 with phosphoric acid.

Sodium stock solutions were prepared from each of the following reagent grade salts by dissolving appropriate amounts in deionized water to give 12,000 ppm sodium: $Na_2SO_4 \cdot 5H_2O$ (J. T. Baker Chemical Co., Phillipsburg, NJ), $NaNO_3$ (Fischer Scientific Co., Fairlawn, NJ) and NaCl, NaH_2PO_4 (Mallinckrodt, Inc., St. Louis, MO).

Potassium stock solutions were prepared from each of the following reagent grade salts by dissolving appropriate amounts in deionized water to give 10,000 ppm potassium: K_2SO_4 (Mallinckrodt, Inc., St. Louis, MO), KNO_3, KCl (J. T. Baker, Phillipsburg, NJ) and KH_2PO_4 (Fischer Scientific Co., Fairlawn, NJ).

A 1000 ppm cesium stock solution was prepared by dissolving 1.2667 grams of reagent grade cesium chloride (J. T. Baker Chemical Co., Phillipsburg, NJ) in 1.00 ℓ of deionized water.

A pooled urine sample was obtained from random specimens and stored at $-20^{\circ}C$ until assayed.

Procedure

Chromium, nickel or selenium working standards were prepared fresh daily from their respective stock solutions in aqueous media and in one of the salt matrices listed in Table 1. The salt concentrations listed represent approximately double the normal levels found in human urine. Nitrate was studied at higher levels since nitric acid is a common matrix modifier for biological samples. A pooled urine sample was also studied to observe the effect of a real matrix on the analyses. When the background from a particular matrix could not be corrected, more dilute solutions were prepared and studied.

Instrumental parameters used for each of the analyte metals are shown in Table 2. Narrow slit widths eliminated stray light and were found to increase detection limits. The recommended heating programs were followed, with the exception of extending the atomization time from 7 sec to 10 sec for chromium and nickel to insure complete

Table 1

Anion and Cation Concentrations in the Matrices Studied

Anions	Cations
12,000 ppm Cl^- (as HCl)	6,000 ppm Na^+ (as NaCl, $NaNO_3$, NaH_2PO_4 or Na_2SO_4)
10,000 ppm NO_3^- (as HNO_3)	5,000 ppm K^+ (as KCl, KNO_3, KH_2PO_4, or K_2SO_4)
8,000 ppm PO_4^{-3} (as H_3PO_4)	500 ppm Ca^{+2} (as $CaCl_2$, $Ca(NO_3)_2$ or $Ca(H_2PO_4)_2$)
8,000 ppm SO_4^{-2} (as H_2SO_4)	500 ppm Mg^{+2} (as $MgCl_2$, $Mg(NO_3)_2$, $Mg(H_2PO_4)_2$ or $MgSO_4$)

Table 2

Instrumental Parameters Used for Chromium, Nickel and Selenium Analyses

	Chromium	Nickel	Selenium
Lamp Current (mA)	12.5	10.0	20.0
Wavelength (nm)	357.9	232.0	196.0
Band Width (nm)	0.2	0.2	0.4
Heating Program (initial temperature, ^{o}C-final temperature, ^{o}C/time,sec)			
Dry	80-120/30	80-120/30	80-120/60
Ash	700-700/30	700-700/30	400-400/30
Atomize	2700-2700/10	2700-2700/10	2400-2400/7
Clean	2800-2800/3	2800-2800/3	2800-2800/3

complete atomization. Nitrogen carrier gas was used at a flow rate of 100 ml/min. The gas interrupt mode was used during atomization. The sample volume for each injection was 10 μl. All injections were made in duplicate, alternating matrix-free samples with matrix-containing samples to prevent apparent effects arising from the accumulation of salts in the furnace or from electronic drift in the baseline. Pyrolytic graphite tube furnaces were used for all determinations.

Chromium was analyzed at 10, 25 and 50 ppb levels. In addition to the salts listed in Table 1, the effect of 500 ppm cesium as the chloride salt on the chromium signal was studied in an effort to investigate the possibility of signal enhancement due to ionization suppression effects seen with sodium and potassium chloride. Because the analysis of chromium in urine has been shown to be dependent on ash temperature (1), the pooled urine matrix was ashed at the standard $700^{\circ}C$ temperature and at the $1200^{\circ}C$ temperature cited as optimal. Nickel was analyzed at 10, 20 and 50 ppb levels.

Selenium was analyzed at 25, 50 and 100 ppb levels. To enhance the absorbance signal, all selenium solutions contained 150 ppm Ni^+ as a matrix modifier (10). The effect of a 10% nitric acid matrix on the suppression of selenium by phosphate, sulfate and chloride was examined.

The various metal-containing solutions were
analyzed by polarized Zeeman atomic absorption spectro-
photometry, using both constant current temperature
control and constant optical emission temperature
control during atomization. The effect of the salt
matrix on the analysis of the metal was determined by
comparing peak area, peak height, appearance time and
peak shape of the aqueous sample to the matrix-containing
sample. Peak areas (integrated absorbance) were
calculated by the instrument's electronic integrator.
Peak heights were measured directly from the recalled
peak as the distance from the baseline to the signal
maximum. Blank values from matrix-containing solutions
without analyte were subtracted from peak area and
height measurements prior to comparison. Changes in
either peak area or height of greater than 10% were
considered to be significant. Appearance times were
measured as the time from the start of atomization to
the signal maximum. Knowledge of chart speed and
atomization interval allowed conversion of appearance
time from millimeters to seconds. Various changes in peak
shape, including multiple peaks, shoulders and dips in
the baseline, were determined by visual inspection of
the signal.

Peak half-widths were examined for the aqueous
standards to determine whether the time constant of the

detector/readout system was adequate. Half-widths were measured as the width of the peak at half the peak's height.

RESULTS AND DISCUSSION

General

      The use of the optical temperature controller
results in faster atomization of the analyte. Theore-
tically, the absorbance signal should be a sharper peak
with the same area as the signal obtained when current
control is used. The appearance time and half-width
should be decreased when optical control is used. Table 3
lists the absorbance signal areas, heights, appearance
times and half-widths for chromium, nickel and selenium.
As predicted, the peak heights were larger and the
appearance times and half-widths were smaller when
optical control was used. Peak areas using the two
types of temperature control were the same, at the 95%
confidence level, in the case of chromium. For nickel,
current control resulted in a slightly lower peak area
value. The lower value is probably due to incomplete
atomization of nickel during the atomization period.
Figure 3 shows the actual recalled signals for an aqueous
50 ppb nickel standard. Under current control conditions,
there is a drop in the nickel signal at the end of the
atomization period indicating incomplete atomization.

Table 3

Comparison of Atomic Absorption Signals for Chromium, Nickel and Selenium
Using Constant Current and Optical Temperature Control

	Area (abs sec)			Height (absorbance)			Appearance Time (sec)			Half-width (msec)		
	Mean	% r.s.d.		Mean	% r.s.d.		Mean	% r.s.d.		Mean	% r.s.d.	
Chromium (25 ppb)												
Current Control	0.137	7.4*	1.8**	0.113	9.3	1.8	4.01	6.7	2.0	2838	5.9	2.7
Optical Control	0.150	7.0	3.0	0.159	8.8	2.7	2.18	5.2	2.2	1100	4.7	4.2
Nickel (50 ppb)												
Current Control	0.125	24	3.0	0.071	22	3.6	4.95	12	2.8	3425	12	2.8
Optical Control	0.164	6.0	2.7	0.125	6.2	2.4	2.33	5.2	2.1	1475	8.1	2.1
Selenium (110 ppb)												
Current Control	0.223	23	1.5	0.053	35	3.2	3.89	12	2.7	1659	27	1.7
Optical Control	0.152	11	1.8	0.159	6.2	1.9	1.37	5.1	2.0	430	14	3.3

*between-run, 5 different days

**within-run, n=10

50 ppb Nickel

OPTICAL CONTROL

Area = 0.142 abs sec

Height = 0.111 abs

Appearance = 2.48 sec

CURRENT CONTROL

Area = 0.132 abs sec

Height = 0.057 abs

Appearance = 4.40 sec

ABSORBANCE, |———| = 0.010 absorbance units

start
atom

start
atom

TIME, |———| = 2.5 seconds
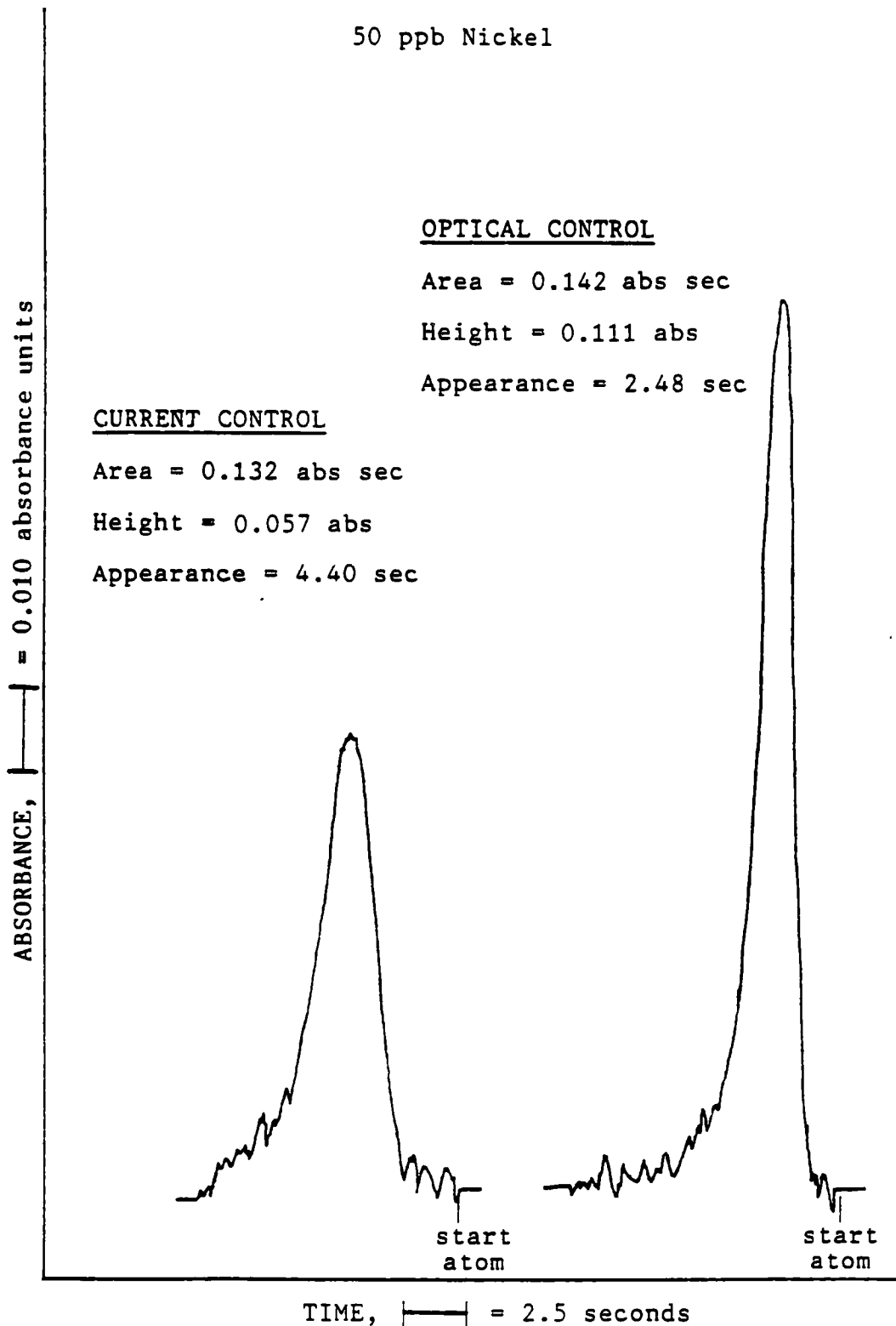
Figure 3. Comparison of the atomic absorption signals
for nickel using current and optical controls

Figure 4 illustrates a similar drop observed when chromium
was analyzed using current control.

The peak area for selenium was higher when current
control was employed. Examination of the actual signals
for selenium in Figure 5 shows the signal obtained under
optical control conditions to be very narrow with a
half-width of 350 msec. To actually record this peak,
the time constant of the detector/readout system must
be 17 msec (one-tenth the half-width divided by two to
account for the detector looking alternately at parallel
and perpendicular source beams). The lower area obtained
under optical control may be explained by an insufficient
time constant of the detector used. Under current
control, the selenium atomizes slowly enough to be more
accurately recorded.

Table 3 also shows the relative, within-run
standard deviation for each analysis. These numbers range
from 1.8-4.2%. The values provided the basis on which
a change of 10% in peak area, peak height or appearance
time was considered to be a significant effect.

The sensitivities and detection limits for the
chromium, nickel and selenium analyses are listed in
Table 4. Values obtained when using both current and
optical controls are given. Sensitivities were calculated
as the quantity of analyte required to give 0.0044
absorbance seconds. The sensitivities of all three

25 ppb Chromium

100 ppb Selenium

OPTICAL CONTROL

Area = 0.148 abs sec

Height = 0.173 abs

Appearance = 1.33 sec

CURRENT CONTROL

Area = 0.182 abs sec

Height = 0.055 abs

Appearance = 4.16 sec

start
atom

start
atom

ABSORBANCE, |⊥| = 0.010 absorbance units
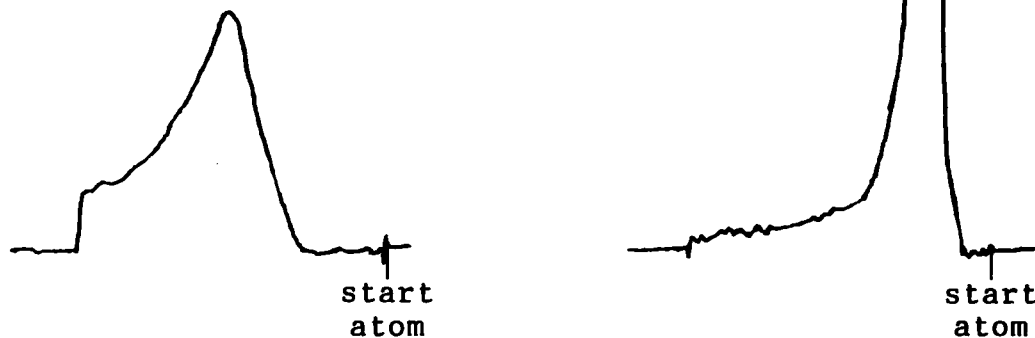
TIME, |————| = 3 seconds
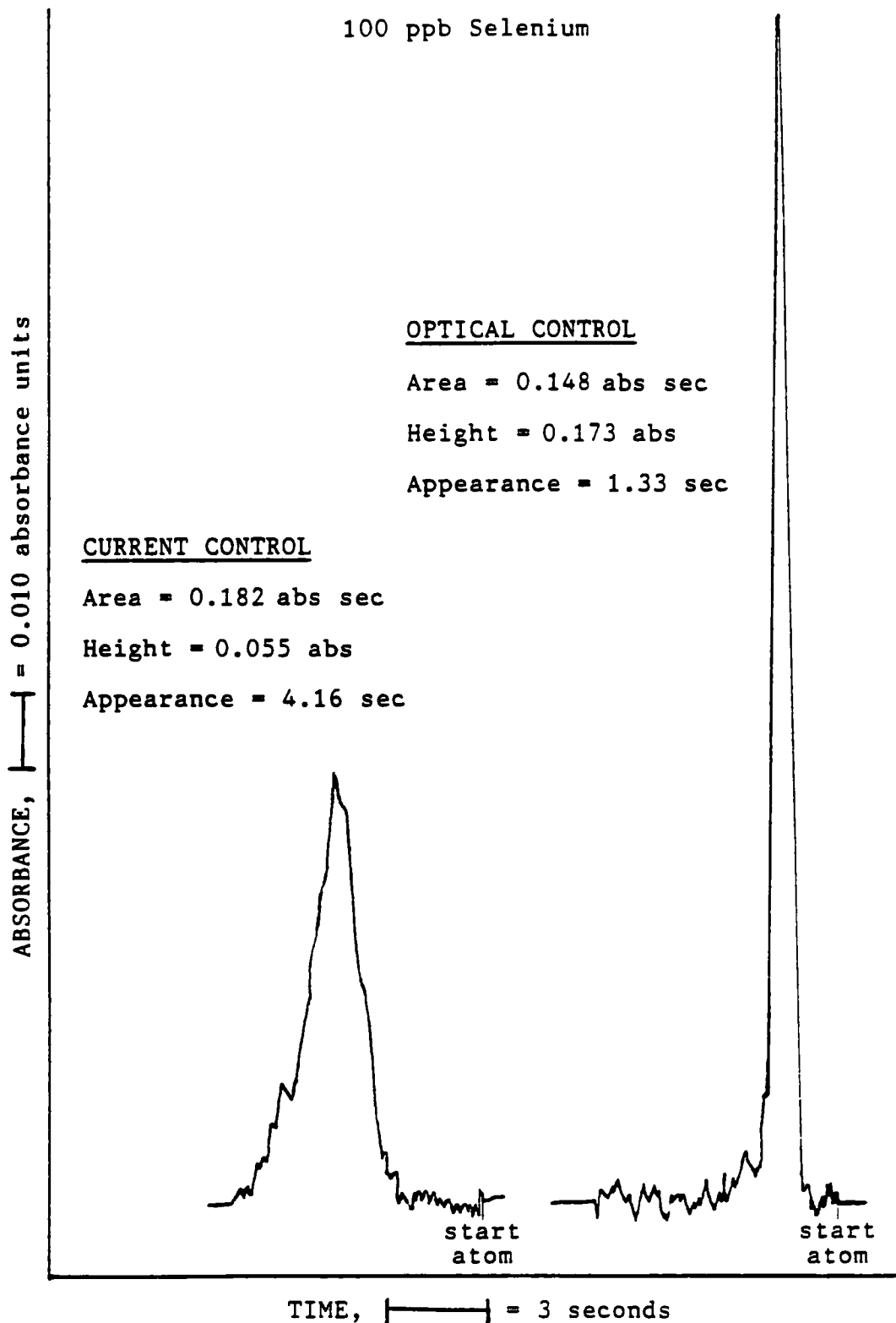
Figure 5 . Comparison of the atomic absorption signals
for selenium using current and optical controls

Table 4

Sensitivity and Detection Limits for Chromium, Nickel and Selenium Analyses

	Sensitivity	Detection Limit (pg)
Chromium		
Current Control	7.6 ± 0.6*	10.0 ± 0.9
Optical Control	8.0 ± 0.6	3.0 ± 0.3
Nickel		
Current Control	15.6 ± 3.7	35.0 ± 0.5
Optical Control	13.3 ± 0.8	14.0 ± 0.3
Selenium		
Current Control	20.8 ± 4.8	120.0 ± 3.8
Optical Control	26.4 ± 2.9	40.0 ± 0.8

*means$\pm$s.d., between-run from 5 runs on different days

$^{+}$pg/0.0044 abs sec

analytes using current control were the same, at a 95%
confidence level, as when optical control was used.
Detection limits were calculated as the mass of analyte
which gave a signal-to-noise ratio of 2. Detection
limits using optical control were improved over
current control by a factor of 3.0 for chromium, a
factor of 2.5 for nickel and a factor of 3.0 for selenium.

Table 5 lists the equations and correlation
coefficients for the standard curves of chromium, nickel
and selenium using current and optical temperature
controls. The six analyses were linear over the concen-
tration ranges studied, with correlation coefficients
significant at the 0.01 level.

Chromium

The basic mechanism of chromium atom formation
has been proposed by several researchers (29, 30). The
formation of the oxide/halide on heating is followed by
carbon reduction to the atomic state:

$$Cr_2O_3(s) \xrightarrow{\text{carbon red}} Cr(s) \xrightarrow{\hspace{2cm}} Cr(g).$$
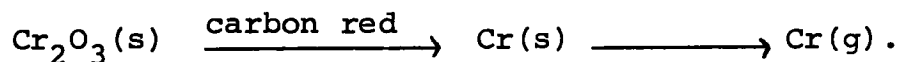
No dimeric chromium species have been observed in the
sequence. Matrix components lead to a change in the
mechanism by affecting the fraction of analyte converted
to free atoms, the rate of atomization or the residence
time of the free atoms in the furnace (31).

The relative effects of the matrices on the chromium signal compared to the aqueous standards are listed in Table 6. The concentrations of sodium sulfate, potassium sulfate and potassium chloride were adjusted from the proposed concentrations to bring background absorbance below 1.7 absorbance-seconds. Pritchard and Reeves (32) attributed the interferences from such salts to non-atomic absorption spectra they produce. Increased ash temperature could have reduced the interference. However, in this work, constant conditions were required for comparison purposes.

Several trends are observed in the data from Table 6. The acids exhibit no effects. The effect of sodium and nitrate seem to be determined by the ion with which they are paired.

Magnesium enhanced the height of the chromium signal. Figure 6 illustrates the effect of magnesium nitrate on the absorbance signal when using optical control. The enhancing effect of magnesium nitrate has been previously documented by Manning and Slavin (33). They attribute the enhancement to the embedding of the analyte in a matrix of magnesium oxide, thus delaying vaporization of the analyte until the magnesium oxide is vaporized. Their explanation is further supported by the fact that the appearance time of the chromium signal is always longer when magnesium is present in the matrix.

Table 6

Relative % Effects of Individual Matrices on the Chromium Signal
Using Both Current and Optical Controls

Matrix	Concentration (ppm) Current/Optical	Area Current/Optical	Height Current/Optical	Appearance Time Current/Optical	Peak Shape Current/Optical
Nitrate (HNO_3)	10,000/10,000	<10/<10	<10/<10	<10/<10	0/0
Chloride (HCl)	12,500/12,500	<10/<10	<10/<10	<10/<10	0/0
Sulfate (H_2SO_4)	8,000/8,000	<10/<10	<10/<10	<10/<10	0/0
Phosphate (H_3PO_4)	8,000/8,000	<10/<10	<10/<10	<10/<10	0/0
Sodium ($NaNO_3$)	6,000/6,000	<10/<10	<10/<10	<10/<10	S/0
Potassium (KNO_3)	5,000/5,000	<10/<10	−19/−11	<10/<10	0/0
Calcium ($Ca(NO_3)_2$)	500/500	+28/+14	+49/+45	−22/−18	DP/S
Magnesium ($Mg(NO_3)_2$)	500/500	<10/<10	+65/+98	+26/+32	V/0
Sodium (NaCl)	6,000/6,000	−71/−86	−74/−86	<10/<10	S/N
Potassium (KCl)	2,500/5,000	−15/−52	−26/−56	<10/<10	N/N
Calcium ($CaCl_2$)	500/500	−10/−23	−16/−40	<10/−27	S/S
Magnesium ($MgCl_2$)	500/500	<10/<10	+25/+61	+12/+44	S/0
Sodium (Na_2SO_4)	1,500/600	−31/−20	−49/−32	<10/<10	S/N
Potassium (K_2SO_4)	2,500/500	−69/−41	−86/−48	<10/<10	N/N
Magnesium ($MgSO_4$)	500/500	<10/<10	<10/−15	+18/+29	0/S
Sodium (NaH_2PO_4)	6,000/6,000	+16/+27	+51/+43	<10/<10	S/S
Potassium (KH_2PO_4)	5,000/5,000	<10/−48	<10/−60	<10/<10	S/S
Calcium ($Ca(H_2PO_4)_2$)	500/500	+10/+16	+32/+35	−21/<10	0/S
Magnesium ($Mg(H_2PO_4)_2$)	500/500	+10/+18	+37/+42	<10/<10	0/0

+ = increase, − = decrease, 0 = no change, DP = double peak, S = shoulder,
V = variable, N = negative dip
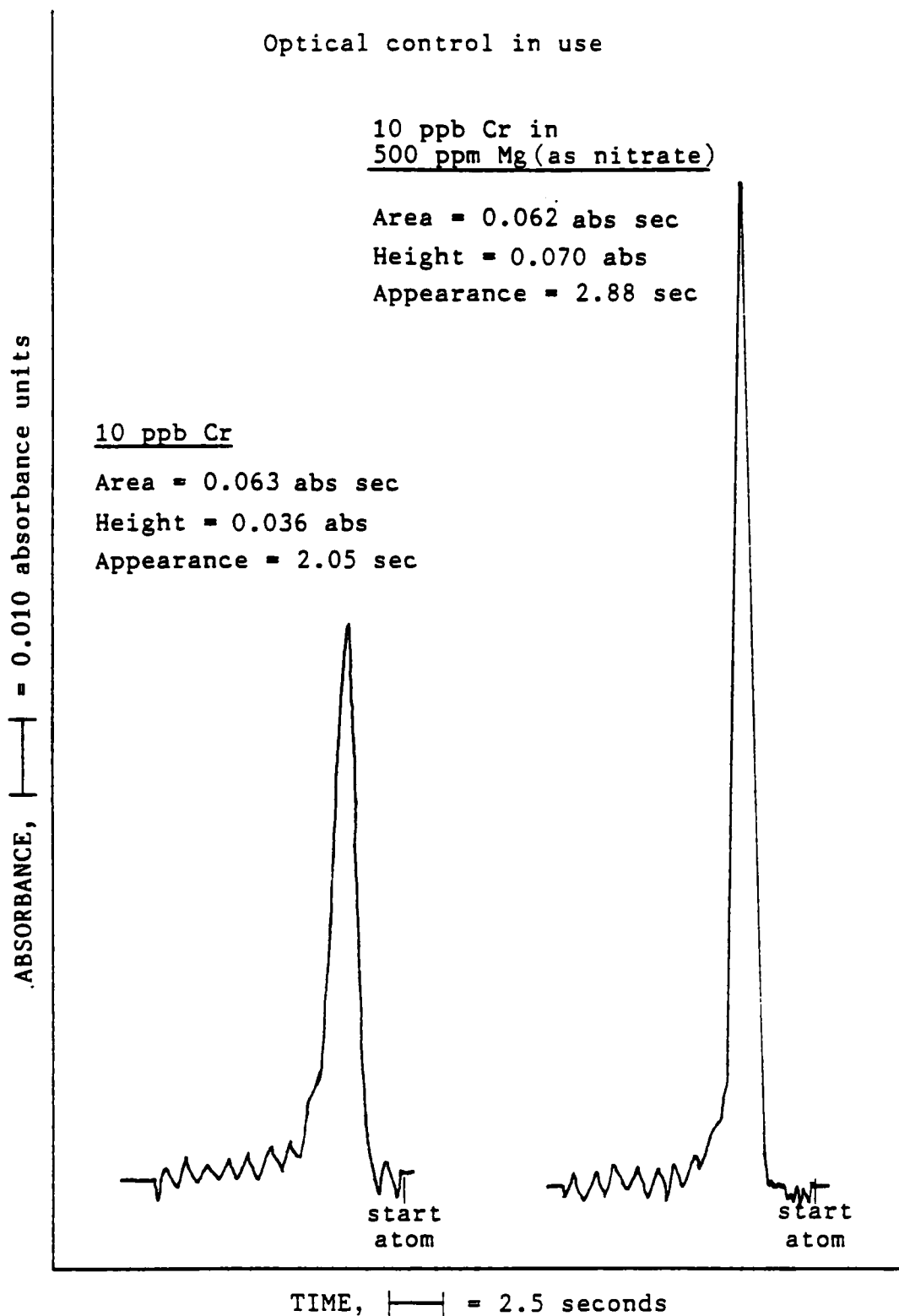
Figure 6 . Comparison of atomic absorption signals for
chromium with and without added magnesium nitrate

An enhancing effect due to calcium nitrate has also been recognized for some time and its use as a matrix modifier for chromium analyses is recommended by EPA (34). Manning and Slavin conclude that calcium nitrate plays a role similar to magnesium nitrate. However, the data from Table 6 shows that calcium enhances both peak area and peak height and that it shortens the appearance time. An atomization mechanism which changes the atomization interval and the rate of atom formation is supported by these data.

Phosphate ion appears to enhance the area and height of the chromium signal. This could be due to the formation of thermally stable chromium phosphate, thus preventing losses during the ash stage and causing the chromium to atomize at a higher temperature.

Potassium, chloride and sulfate suppress the chromium signal. The reason for suppression by potassium cannot be explained at present. Chloride probably combines with chromium to form volatile chromium chlorides which are lost during ashing. The absence of signal suppression when hydrochloric acid was present could be due to the acid evaporating during the dry stage (b.p. azeotropic HCl in water: $(108^{\circ}C)$.

The interference by sulfate is probably best explained by the formation of the diatomic species, S_2, during atomization (35). S_2 and other such species have

rotational quantum transitions which are perturbed in a magnetic field resulting in a Zeeman spectrum (36). Massman has shown that background due to such line-rich electronic excitation spectra is not properly corrected by the Polarized Zeeman correction system (37). The measured background is generally greater than the real background absorbance. This may also explain the negative dips observed in the baseline when sodium sulfate, potassium sulfate and magnesium sulfate were present. The absence of signal suppression and a negative dip in the baseline when sulfuric acid was present could be due to the acid evaporating during the ash stage (b.p. H_2SO_4:290°C).

The negative dip in the baseline observed when sodium and potassium chloride were present remains unexplained. Figure 7 illustrates the signal suppression and dip in the baseline caused by sodium chloride.

Shoulders and double peaks were observed in the chromium signal with all the nitrate salts and with dosium and potassium phosphate. Figure 8 illustrates the double peak and shoulder seen when sodium and potassium phosphate were present, respectively. These phenomena suggest that more than one chromium species has been formed, each being atomized at a different temperature. Veillon and co-workers (38) showed that

Optical control in use

10 ppb Cr in
6000 ppm Na (as chloride)

Area = 0.009 abs sec

Height = 0.014 abs

Appearance = 2.22 sec

10 ppb Cr

Area = 0.058 abs sec

Height = 0.069 abs

Appearance = 2.22 sec

start
atom

start
atom

ABSORBANCE, = 0.010 absorbance units

TIME, |——| = 2.5 seconds

34
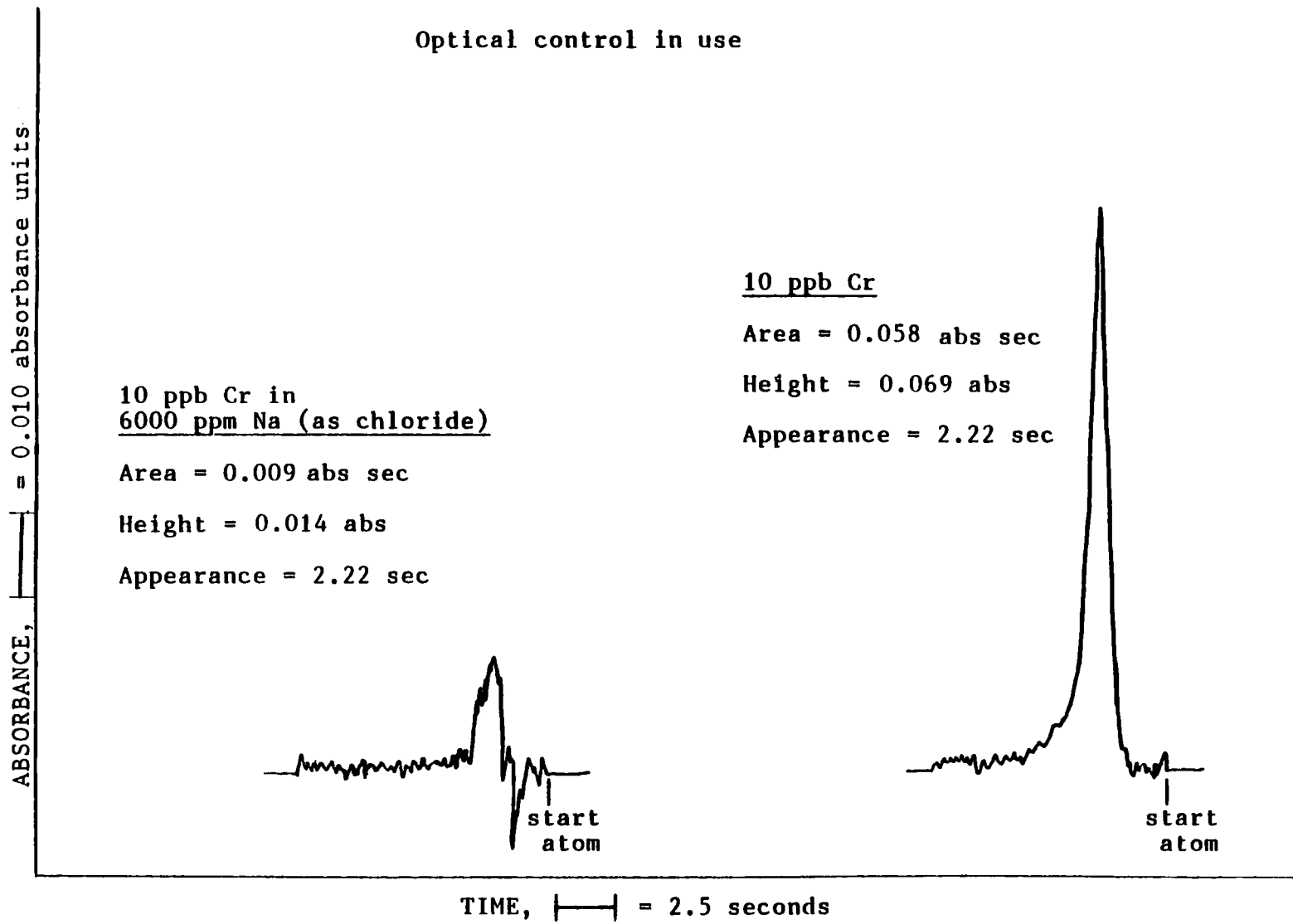
Optical control in use

10 ppb Cr in
5000 ppm K (as phosphate)

10 ppb Cr in
6000 ppm Na (as phosphate)

ABSORBANCE, ▮ = 0.010 absorbance units

start
atom

start
atom
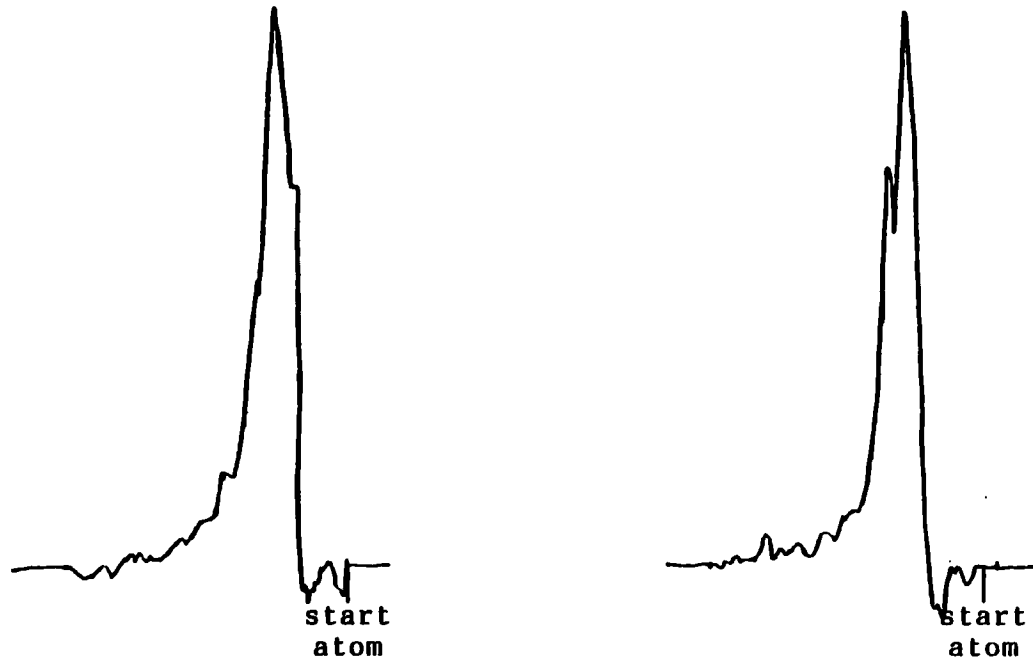
TIME, ├───┤ = 2.5 seconds
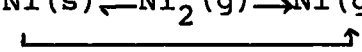
carbide formation on the furnace wall results in a discontinuous release of chromium during subsequent atomizations. Gas phase species may also be formed by interaction of chromium with nitrogen purge gas.

When ions with opposing effects were present in the matrix, a "cancelling out" appeared to take place. For example, when magnesium and sulfate were both present in the form of magnesium sulfate, the net effect on the peak area and height was zero. However, the appearance time was still increased due to the presence of magnesium, indicating that the same mechanism of volatilization (trapping in a magnesium oxide matrix) may be occurring. Similar interactions seemed to occur when calcium chloride, magnesium chloride, potassium nitrate and potassium phosphate were present in the matrix. In these matrices the net effect was not zero, with one of the ions apparently exerting a stronger effect.

It has been suggested that the enhancement of the chromium signal by calcium and magnesium could also be due to suppression of analyte ionization. Calcium and magnesium act as deionizers by increasing the partial pressure of free electrons in the furnace. Analyte ionization has been studied in standard graphite furnaces. Sturgeon and Berman (39) showed ionization to be negligible when the ionization potential of the analyte is greater than 4.6 eV. In addition, insertion

of temperature-corrected electronic partition functions
(40) into the Saha equation yields a small degree of
ionization equal to 0.0036. However, the effect of the
magnetic field on ionization in the PZAA systems has
not been considered. The possibility that calcium and
magnesium enhance the chromium signal via an ionization
suppression mechanism was tested by analyzing chromium in
a cesium chloride matrix. No enhancement of the chromium
signal was observed. Thus, it was concluded that calcium
and magnesium do not act via an ionization suppression.

Nickel

The basic mechanism of nickel atom formation is
more complicated than that for chromium due to the
existence of a nickel dimeric species (29). The reduction
of nickel oxide to solid nickel metal may be followed by
formation upon evaporation of monomeric nickel atoms or
the dimeric nickel species: $NiO(s) \longrightarrow Ni(s) \rightleftharpoons Ni_2(g) \rightarrow Ni(g)$.

The relative effects of the salt matrices on the
nickel signal compared to the aqueous standards are
listed in Table 7. In order to obtain proper background
correction, one-tenth of the proposed concentrations
of sodium and potassium chloride, sulfate and phosphate
salts was studied. Since the slit width for the nickel
analyses was the same as for the chromium analyses, the

Table 7

Relative % Effects of Individual Matrices on the Nickel Signal
Using Both Current and Optical Controls

Matrix	Concentration (ppm) Current/Optical	Area Current/Optical	Height Current/Optical	Appearance Time Current/Optical	Peak Shape Current/Optical
Nitrate (HNO_3)	10,000/10,000	-18/-12	-18/-21	<10/<10	0/0
Chloride (HCl)	12,500/12,500	<10/<10	<10/<10	<10/<10	0/0
Sulfate (H_2SO_4)	8,000/8,000	<10/<10	<10/<10	<10/<10	0/0
Phosphate (H_3PO_4)	6,000/6,000	<10/-16	<10/<10	<10/<10	0/0
Sodium ($NaNO_3$)	5,000/5,000	-26/<10	-28/-18	<10/<10	0/0
Potassium (KNO_3)	500/500	-16/<10	-21/<10	<10/<10	0/0
Calcium ($Ca(NO_3)_2$)	500/500	<10/<10	<10/<10	<10/<10	0/0
Magnesium ($Mg(NO_3)_2$)	600/600	+10/<10	+10/<10	<10/<10	0/0
Sodium (NaCl)	500/500	<10/<10	<10/<10	<10/<10	0/0
Potassium (KCl)	500/500	<10/<10	+13/<10	<10/<10	0/0
Calcium ($CaCl_2$)	500/500	<10/<10	-16/-10	<10/<10	0/0
Magnesium ($MgCl_2$)	500/500	+14/+16	+14/+17	<10/<10	0/0
Sodium (Na_2SO_4)	600/600	<10/<10	-18/<10	<10/<10	0/S
Potassium (K_2SO_4)	500/500	-41/-16	-25/-18	<10/<10	0/0
Magnesium ($MgSO_4$)	500/500	+26/+13	+38/+61	+26/+13	0/0
Sodium (NaH_2PO_4)	600/600	<10/+19	<10/<10	<10/<10	0/S
Potassium (KH_2PO_4)	500/500	<10/<10	<10/<10	<10/<10	0/0
Calcium ($Ca(HPO_4)_2$)	500/500	<10/+10	+10/+20	<10/<10	0/0
Magnesium ($Mg(HPO_4)_2$)	500/500	<10/<10	<10/<10	<10/<10	0/0

+ = increase, - = decrease, 0 = no change, DP = double peak, S = shoulder,
V = variable, N = negative dip

high absorbance exhibited by these salts is probably
due to molecular absorption at the nickel wavelength.
This is further supported by the fact that when lower
concentrations of the salts were present, no effects
were observed in the absorbance signal.

Fewer interferences by matrix components were
observed for the nickel analyses than for chromium. The
acids (except for nitric), calcium nitrate, sodium
chloride, potassium chloride, potassium phosphate and
magnesium phosphate exhibited no effects. The obvious
trends seen in Table 7 are the enhancement due to
magnesium and the suppression due to nitrate. Also,
potassium and sulfate seem to suppress the signal while
phosphate seems to slightly enhance it.

Enhancement of the nickel signal due to magnesium
is probably a result of the same process described for
chromium, that of embedding the analyte in a matrix of
magnesium oxide, thus delaying atomization and preventing
losses during ashing.

The best explanation for the suppression effects
of nitrate and sulfate on the nickel signal is the
formation of polyatomic species such as NO, NS and SO_2,
which exhibit structured background in the region of
the nickel analytical wavelength and produce Zeeman
spectra in a magnetic field. The lack of negative
dips in the baseline of the nickel signal which were

seen with chromium could be due to the interference occurring simultaneously with the signal.

The suppression by potassium and enhancement by phosphate do not have obvious explanations.

The appearance time of the nickel signal was altered in only one instance. Magnesium sulfate caused slower atomization.

Shoulders on the absorbance signals were seen when calcium nitrate and sodium sulfate were the matrix components, indicating that more than one nickel species was formed during atomization. Also, physical entrapment of nickel in the matrix could cause uneven atomization, resulting in shoulders on absorbance signals.

Selenium

No mechanism has been proposed to describe the atomization of selenium in the graphite furnace.

The relative effects of the salt matrices on the selenium signal compared to the aqueous standards are listed in Table 8. Due to background absorbances greater than 1.7, most of the salts could not be analyzed at the proposed concentrations. The adjusted concentrations are indicated in the table.

Nitric acid, sodium chloride and potassium chloride exhibit no effects on the selenium signal. Magnesium nitrate and calcium chloride caused an increase

Table 8

Relative % Effects of Individual Matrices on the Selenium Signal
Using Both Current and Optical Controls

Matrix	Concentration (ppm) Current/Optical	Area Current/Optical	Height Current/Optical	Appearance Time Current/Optical	Peak Shape Current/Optical
Nitrate (HNO_3)	10,000/10,000	<10/<10	<10/<10	<10/<10	0/0
Chloride (HCl)	12,500/12,500	-10/-19	-18/-28	<10/<10	0/0
Sulfate (H_2SO_4)	500/1,000	-74/-81	-97/-90	?/<10	?/0
Phosphate (H_3PO_4)	1,000/1,000	-100/-47	-100/-68	?/-19	?/0
Sodium ($NaNO_3$)	600/600	-12/-92	-29/-79	<10/<10	N/N
Potassium (KNO_3)	500/500	-15/-73	<10/-75	<10/-10	N/N
Calcium ($Ca(NO_3)_2$)	500/500	-24/-29	<10/-25	+12/+16	0/0
Magnesium ($Mg(NO_3)_2$)	500/500	<10/<10	+24/+16	+16/+15	0/0
Sodium (NaCl)	60/60	<10/<10	<10/<10	<10/<10	0/0
Potassium (KCl)	50/50	<10/<10	<10/<10	<10/<10	0/0
Calcium ($CaCl_2$)	500/500	-14/<10	+37/+23	<10/<10	0/0
Magnesium ($MgCl_2$)	500/500	<10/<10	<10/-14	+14/<10	0/0
Sodium (Na_2SO_4)	60/60	-59/-27	-58/-30	-14/-8	0/0
Potassium (K_2SO_4)	50/50	-67/-31	-59/-31	-15/-10	0/0
Magnesium ($MgSO_4$)	50/50	-30/-32	-12/-13	-11/<10	S/S
Sodium (NaH_2PO_4)	60/60	-38/-47	-34/-52	-23/-18	0/0
Potassium (KH_2PO_4)	50/50	-10/-13	<10/<10	-17/-12	0/0
Calcium ($Ca(HPO_4)_2$)	50/50	-42/-41	-46/-47	<10/<10	DP/DP
Magnesium ($Mg(HPO_4)_2$)	50/50	-68/-64	-68/-76	-32/-42	0/V

+ = increase, - = decrease, 0 = no change, DP = double peak, S = shoulder, V = variable,
N = negative dip

in the signal height, probably acting in a manner
similar to chromium and nickel. All of the other salts
studied severely suppressed the signal.

The suppression of the selenium signal by the
various salts is most likely due to spectral inter-
ferences by polyatomic species formed in the furnace.
A number of polyatomic molecules absorb near the selenium
analytical wavelength. Martinsen and Langmyhr (35)
found that selenium analyses were highly subject to
spectral interferences from CS, COS, S_2 and SO_2 when
sulfuric acid was present. Sulfate salts could produce
the same species. Likewise, thermal decomposition of
phosphate has been found to produce PO and P_2 which
cause spectral interferences on the selenium analyses
(41). Nitrate salts could produce NO which has an
absorption at 196.1 nm (42).

The appearance time of selenium was delayed when
calcium nitrate, magnesium nitrate and magnesium
chloride were present. The atomization of selenium
was more rapid when phosphate (except for calcium
phosphate) or sulfate was present.

Negative dips in the baseline occurred when
sodium nitrate and potassium nitrate were present, even
in the unspiked matrix, further supporting the thought
that nitrate interference is spectral in origin.

Shoulders and double peaks were observed with calcium phosphate, magnesium phosphate and magnesium sulfate.

Addition of 10% nitric acid to the hydrochloric, phosphoric and sulfuric acid matrices had no effect on the suppression caused by these anions.

Urine

Table 9 lists the relative effects of the urine matrix on the analysis of chromium, nickel and selenium. The optical temperature controller was used for increased sensitivity.

Peak area and peak height were suppressed for all three metals when analyzed in urine. The appearance times were not altered in any of the three cases. Negative dips in the baseline were observed for nickel and selenium when urine was present. These results cannot be directly correlated to the matrix studies performed. In addition to inorganic salts, urine contains several organic compounds, including uric acid and oxalic acid. Better analytical results could be obtained by optimizing instrumental conditions for actual urine samples. For example, a higher ash temperature could remove some of the interferences to the selenium analyses.

Whether the ash temperature was $700^{\circ}C$ or $1200^{\circ}C$, identical results were obtained when chromium was analyzed in urine. However, the higher ash temperature

Table 9

Effect of a Urine Matrix on the Atomic Absorption Signals of Chromium, Nickel and Selenium Using Optical Temperature Control

	Chromium	Nickel	Selenium
Urine Dilution	1:2	1:4	1:4
Background Absorbance	0.025 abs sec	0.767 abs sec	0.837 abs sec
Effect on Peak Area	-22%	-14%	-76%
Effect on Peak Height	-32%	-27%	-87%
Effect on Appearance Time	<10%	<10%	<10%
Effect on Peak Shape	0	N	N

*- = decrease; 0 = no change; N = negative dip

resulted in a faster appearance time than the lower ash temperature (2.95 sec vs. 2.16 sec). This was most likely due to matrix components which delay atomization being driven off in the ash stage.

CONCLUSIONS

Manning and Slavin (33) have proposed direct
methods of analyzing metals in natural waters by atomic
absorption spectrometry with the following recommenda-
tions: atomizing at a stabilized temperature, using
pyrolytic tubes, having a fast recorder response,
evaluating the signal area rather than peak height,
using matrix modifiers and using PZAA if high background
is not removed by ashing. The present study followed
these recommendations, with the exception of atomizing
at a stabilized temperature, and found that chromium,
nickel and selenium could not be analyzed directly in
urine.

The rate of furnace heating was found to affect
sensitivity. The faster rate of heating provided by
optical temperature control increased sensitivity and
should probably lengthen furnace life due to the shorter
atomization times required. The matrix effects observed
were similar whether optical control or current control
was used.

The importance of an adequate detector/readout
response time was realized when selenium was analyzed
with optical temperature control. The sharp signal

46

obtained had a smaller area than when current control was used indicating that the selenium atomized too quickly for the instrument to accurately record the signal. The response time appeared to be adequate for the other analyses performed.

Slightly fewer interference effects were found in analyte signal areas versus signal heights. However, since signal areas were significantly altered by matrix salts, no justification could be made for using area to evaluate analyte concentrations in lieu of standard additions.

High concentrations of sodium and potassium salts required the urine to be diluted to attain proper background correction. More suitable matrix modifiers could alleviate this problem. The enhancement effects observed when particular matrix salts were present suggest potential modifiers for the analytes. Calcium and magnesium nitrate and calcium, magnesium and sodium phosphate enhanced the chromium signal. Magnesium chloride and magnesium sulfate enhanced the nickel signal. Magnesium nitrate enhanced the selenium signal.

This work verified that complex reactions in the graphite furnace and atomization behaviour of metals are not predictable. It was noted that calcium and magnesium, although chemically similar cations, act to enhance the absorption signals of the analytes via

different mechanisms. The possibility that calcium and magnesium enhance the signals via ionization suppression of the analyte was shown to be an unlikely mechanism.

Suppression of analyte signals by a number of ions was observed. Potassium, sulfate and nitrate were found to suppress nickel signals. Potassium, sulfate and chloride were found to suppress chromium signals. Phosphate, sulfate and nitrate were found to suppress selenium signals.

A spectral interference unique to the Polarized Zeeman background correction system could be the cause of many of the suppression effects by anions. Anions such as phosphate, sulfate and nitrate decompose in the furnace to form polyatomic species which produce Zeeman spectra. Massman (37) showed that the structured background from such species cause negative deviations in absorbance signals. The decreases in signal area and height and the negative dips in peak shape observed in this study are in agreement with Massman's findings. S_2 has absorption lines which might interfere at the chromium analytical wavelength. NO, NS and SO_2 have absorption lines which could interfere at the nickel wavelength. CS, COS, S_2, SO_2, PO, P_2 and NO have absorption lines which could interfere at the selenium wavelength.

Not all the matrix effects have explanations at present. Further investigation of the thermochemical reactions in the furnace must be performed to fully interpret the results of interference studies such as this one.

BIBLIOGRAPHY

1. Veillon, C., Patterson, K. Y. and Bryden, N. A.
   Chromium in Urine as Measured by Atomic Absorption
   Spectrometry. Clin. Chem., Vol. 28, No. 11, 2309-
   2311 (1982).

2. Sunderman, F. W. Measurements of Nickel in
   Biological Materials by Atomic Absorption Spectro-
   metry, Amer. J. Clin. Path., Vol. 44, 182-188 (1965).

3. Hojo, Y. Single-Void Urine Selenium Level Expressed
   in Terms of Creatine Content as an Effective and
   Convenient Indicator of Human Selenium Status. Bull.
   Environ. Contamination Toxicology, Vol. 29, 37-42
   (1982).

4. Hendrikx-Jongerius, G. and de Galan, L. Practical
   Approach to Background Correction and Temperature
   Programming in Graphite Furnace Atomic Absorption
   Spectrometry. Anal. Chim. Acta, Vol. 87, 259-271
   (1976).

5. Koisumi, H., Yasuda, K. and Katayama, M. Atomic
   Absorption Spectrophotometry Based on the Polariza-
   tion Characteristics of the Zeeman Effect. Anal.
   Chem., Vol. 48, No. 8, 1106-1112 (1977).

6. Brown, S. D. Zeeman Effect-Based Background Correction in Atomic Absorption Spectrometry. Anal. Chem., Vol. 49, No. 14, 1269-1277 (1977).

7. Lundberg, E. and Frech, W. Influence of Instrumental Response Time on Interference Effects in Graphite Furnace Atomic Absorption Spectrometry. Anal. Chem., Vol. 53, No. 9, 1437-1442 (1981).

8. Van den Broek, Wim M. G. T. and de Galan, L. Supply and Removal of Sample Vapor in Graphite Thermal Atomizers. Anal. Chem., Vol. 49, No. 14, 2176-2186 (1977).

9. Dolinsek, F. and Stupar, J. Application of the Carbon Cup Atomisation Technique in Water Analysis by Atomic-absorption Spectroscopy. Analyst, Vol. 98, No. 1173, 841-850 (1973).

10. Stein, V. B., Canelli, E. and Richards, A. H. Determination of Dissolved Selenium in Fresh and Estuarine Waters by Flameless Atomic Absorption. Atomic Spectroscopy, Vol. 1, No. 3, 61-65 (1980).

11. Thompson, D. D. and Allen, R. J. Rapid Determination of Selenium in Nutritional Supplements by a Flameless Atomic Absorption Technique Using a Novel Sample Preparation. Atomic Spectroscopy, Vol. 2, No. 2, 53-58 (1981).

12. Szydlowski, F. J. and Vianzon, F. R. Further Studies on the Determination of Selenium Using Graphite

Furnace Atomic Absorption Spectroscopy. Atomic
Spectroscopy, Vol. 1, 39-40 (1980).

13. Chakraborti, D., De Jonghe, W. and Adams, F. The
Determination of Arsenic by Electrothermal Atomic
Absorption Spectrometry with a Graphite Furnace.
Anal. Chim. Acta, 119, 331-340 (1980).

14. Alder, J. F. and Hickman, D. A. The Influence of
Mineral Acid and Hydrogen Peroxide Matrices on
Elemental Sensitivity in Graphite Furnace Atomic
Absorption Spectrometry. Atomic Absorption News-
letter, Vol. 16, No. 4, 110-111 (1977).

15. Sedykh, E. M., Belyaev, Yu. I. and Sorokina, E. V.
Matrix Effect During Electrothermal Atomic Absorption
Determination of Silver, Tellurium, Lead, Cobalt,
Nickel in Materials of Complex Composition. Zh.
Anal. Khim., 35, 2162-2169 (1980).

16. Czobik, E. J. and Matousek, J. P. Interference
Effects in Furnace Atomic Absorption Spectrometry.
Anal. Chem., Vol. 50, No. 1, 2-9 (1978).

17. Tonini, C. Matrix Effects on the Determination of
Some Metals Using Flameless Atomic Spectroscopy.
Tinctoria, Vol. 74, No. 5, 167-169 (1977).

18. Vollkopf, U., Grobenski, Z. and Welz, B. Deter-
mination of Nickel in Serum Using Graphite Furnace
Atomic Absorption. Atomic Spectroscopy, Vol. 2,
No. 2, 68-70 (1981).

19. Beaty, M. and Barnett, W. Techniques for Analyzing Difficult Samples with the HGA Graphite Furnace. Atomic Spectroscopy, Vol. 1, No. 3, 72-77 (1980).

20. Hinderberger, E. J., Kaiser, M. L. and Koirtyohann, S. R. Furnace Atomic Absorption Analysis of Biological Samples Using the L'vov Platform and Matrix Modification. Atomic Spectroscopy, Vol. 2, No. 1, 1-7 (1981).

21. Krasowski, J. A. and Copeland, T. R. Matrix Interference in Furnace Atomic Absorption Spectrometry. Anal. Chem., Vol. 51, No. 11, 1843-1849 (1979).

22. Pleban, P. A. and Pearson, K. H. Determination of Lead in Whole Blood and Urine Using Zeeman Effect Flameless Atomic Absorption Spectroscopy. Anal. Letters, 12, 935-950 (1979).

23. Pleban, P. A. and Pearson, K. H. Determination of Cadmium in Whole Blood and Urine by Zeeman Atomic Absorption Spectroscopy. Clin. Chim. Acta, 99, 267-277 (1979).

24. Koizumi, H. and Yasuda, K. An Application of the Zeeman Effect to Atomic Absorption Spectrometry: A New Method for Background Correction. Spectochim. Acta, Vol. 31B, 237-255 (1976).

25. Frigieri, P. and Trucco, R. The Use of the Zeeman Effect for the Background Correction in Atomic

Absorption Analysis of Biological Fluids.
Spectrochim. Acta, Vol. 35B, 113-118 (1979).

26. Guthrie, B. E., Wolf, W. R. and Weillon, C. Background Correction and Related Problems in the Determination of Chromium in Urine by Graphite Furnace Atomic Absorption Spectrometry. Anal. Chem., Vol. 50, No. 13, 1900-1902 (1978).

27. Vickrey, T. M. and Buren, M. S. Factors Affecting Selenium Atomization Efficiency in Graphite Furnace Atomic Absorption. Anal. Letters, 13, 1465-1485 (1980).

28. Smeyers-Verbeke, J., Michotte, Y. and Massart, D. L. Influence of Some Matrix Elements on the Determination of Copper and Manganese by Furnace Atomic Absorption Spectrometry. Anal. Chem., Vol. 50, No. 1, 10-12 (1978).

29. Sturgeon, R. E., Chakrabarti, C. L. and Langford, C. H. Studies on the Mechanism of Atom Formation in Graphite Furnace Atomic Absorption Spectrometry. Anal. Chem., Vol. 48, No. 12, 1792-1807 (1976).

30. L'vov, B. V., Bayunov, P. A. and Ryabchuk, G. N. A Macrokinetic Theory of Sample Vaporization in Electro-Thermal Atomic Absorption Spectrometry. Spectrochim. Acta, Vol. 36B, No. 5, 397-425 (1981).

31. Maessen, F., Balke, J. and Massee, R. Non-Spectral Interferences in Flameless Atomic Absorption Spectrometry Using Mini-Tube Furnaces. Spectrochim. Acta, Vol. 33B, 311-324 (1978).

32. Pritchard, M. W. and Reeves, R. B. Non-atomic Absorption from Matrix Salts Volatilized from Graphite Atomizers in Atomic Absorption Spectrometry. Anal. Chim. Acta, Vol. 82, 103-111 (1976).

33. Manning, D. C. and Slavin, W. The Determination of Trace Elements in Natural Waters Using the Stabilized Temperature Platform Furnace. Applied Spectroscopy, Vol. 37, No. 1, 1-10 (1982).

34. Methods for the Chemical Analyses of Water and Wastes, EPA-600, 4-79-020 (Environmental Monitoring and Support Laboratory, Cincinnati, OH, 1979).

35. Martinsen, I. and Langmyhr, F. J. Some Observations of the Sulfuric Acid Reactions in Electrothermal Atomic Absorption Spectroscopy with Graphite Furnaces. Anal. Chim. Acta, Vol. 135, 137-143 (1982).

36. Jen, C. K. Rotational Magnetic Moments in Polyatomic Molecules. Physical Review, Vol. 81, No. 2, 197-203 (1951).

37. Massman, H. The Origin of Systematic Errors in Background Measurement in Zeeman Atomic Absorption Spectrometry. Talanta, Vol. 29, 1051-1059 (1982).

38. Veillon, C., Guthrie, B. and Wolf, W.   Retention of
    Chromium by Graphite Furnace Tubes. Anal. Chem.,
    Vol. 52, 457-459 (1980).

39. Sturgeon, R. E. and Berman, S. S.   Microwave
    Attenuation of Electron Concentrations in Graphite
    and Tantalum Tube Electrothermal Atomizers.
    Anal. Chem., Vol. 52, 1049-1053 (1980).

40. De Galan, L., Smith, R. and Winefordner, J. D.
    The Electronic Partition Functions of Atoms and Ions
    Between $1500^{O}K$ and $7000^{O}K$. Spectrochim. Acta,
    Part B, Vol. 23, 521-525 (1968).

41. Saaed, K. and Thomassen, Y. Spectral Interferences
    from Phosphate Matrices in the Determination of
    Antimony, Arsenic, Selenium and Tellurium by
    Electrothermal Atomic Absorption Spectrometry.
    Anal. Chim. Acta, Vol. 130, 281-287 (1981).

42. Pearse, R. W. B. and Gaydon, A. G.   The Identification
    of Molecular Spectra, 3rd Ed., John Wiley and Sons,
    Inc., New York (1963).